

Analysis of the Protein Kinase A-Regulated Proteome of *Cryptococcus neoformans* Identifies a Role for the Ubiquitin-Proteasome Pathway in Capsule Formation

J. M. H. Geddes,^a M. Caza,^b D. Croll,^{b*} N. Stoynov,^c L. J. Foster,^c J. W. Kronstad^{a,b}

Department of Microbiology and Immunology, University of British Columbia, Vancouver, BC, Canada^a; Michael Smith Laboratories, University of British Columbia, Vancouver, BC, Canada^b; Centre for High-throughput Biology, University of British Columbia, Vancouver, BC, Canada^c

* Present address: D. Croll, Institute of Integrative Biology, ETH Zürich, Zürich, Switzerland.

ABSTRACT The opportunistic fungal pathogen *Cryptococcus neoformans* causes life-threatening meningitis in immunocompromised individuals. The expression of virulence factors, including capsule and melanin, is in part regulated by the cyclic-AMP/protein kinase A (cAMP/PKA) signal transduction pathway. In this study, we investigated the influence of PKA on the composition of the intracellular proteome to obtain a comprehensive understanding of the regulation that underpins virulence. Through quantitative proteomics, enrichment and bioinformatic analyses, and an interactome study, we uncovered a pattern of PKA regulation for proteins associated with translation, the proteasome, metabolism, amino acid biosynthesis, and virulence-related functions. PKA regulation of the ubiquitin-proteasome pathway in *C. neoformans* showed a striking parallel with connections between PKA and protein degradation in chronic neurodegenerative disorders and other human diseases. Further investigation of proteasome function with the inhibitor bortezomib revealed an impact on capsule production as well as hypersusceptibility for strains with altered expression or activity of PKA. Parallel studies with tunicamycin also linked endoplasmic reticulum stress with capsule production and PKA. Taken together, the data suggest a model whereby expression of PKA regulatory and catalytic subunits and the activation of PKA influence proteostasis and the function of the endoplasmic reticulum to control the elaboration of the polysaccharide capsule. Overall, this study revealed both broad and conserved influences of the cAMP/PKA pathway on the proteome and identified proteostasis as a potential therapeutic target for the treatment of cryptococcosis.

IMPORTANCE Fungi cause life-threatening diseases, but very few drugs are available to effectively treat fungal infections. The pathogenic fungus *Cryptococcus neoformans* causes a substantial global burden of life-threatening meningitis in patients suffering from HIV/AIDS. An understanding of the mechanisms by which fungi deploy virulence factors to cause disease is critical for developing new therapeutic approaches. We employed a quantitative proteomic approach to define the changes in the protein complement that occur upon modulating the cAMP signaling pathway that regulates virulence in *C. neoformans*. This approach identified a conserved role for cAMP signaling in the regulation of the ubiquitin-proteasome pathway and revealed a link between this pathway and elaboration of a major virulence determinant, the polysaccharide capsule. Targeting the ubiquitin-proteasome pathway opens new therapeutic options for the treatment of cryptococcosis.

Received 27 October 2015 Accepted 9 November 2015 Published 12 January 2016

Citation Geddes JMH, Caza M, Croll D, Stoynov N, Foster LJ, Kronstad JW. 2016. Analysis of the protein kinase A-regulated proteome of *Cryptococcus neoformans* identifies a role for the ubiquitin-proteasome pathway in capsule formation. *mBio* 7(1):e01862-15. doi:10.1128/mBio.01862-15.

Invited Editor Andrew Alspaugh, Duke University Medical Center **Editor** Françoise Dromer, Institut Pasteur

Copyright © 2016 Geddes et al. This is an open-access article distributed under the terms of the [Creative Commons Attribution-Noncommercial-ShareAlike 3.0 Unported license](https://creativecommons.org/licenses/by-nc-sa/4.0/), which permits unrestricted noncommercial use, distribution, and reproduction in any medium, provided the original author and source are credited.

Address correspondence to J. W. Kronstad, kronstad@mssl.ubc.ca.

This article is a direct contribution from a Fellow of the American Academy of Microbiology.

The opportunistic fungal pathogen *Cryptococcus neoformans* causes cryptococcal meningitis in immunocompromised individuals, with a high level of morbidity and mortality in patients suffering from HIV/AIDS (1, 2). The virulence of the fungus is attributed to its ability to grow at 37°C, to produce a polysaccharide capsule and melanin, and to secrete extracellular enzymes and proteins that facilitate proliferation within the host (3–8). The capsule is a major virulence factor, and the constituent polysaccharides are synthesized intracellularly, exported to the cell surface, and attached to the cell wall to contribute immunomodulatory and antiphagocytic properties during infection (9–15). In

C. neoformans, the cyclic-AMP/protein kinase A (cAMP/PKA) signal transduction pathway is a key regulator of virulence factor elaboration and may also regulate the trafficking of virulence components to the cell surface (16). In particular, PKA activity is known to regulate capsule production and melanin formation (17–21). Environmental signals, such as exogenous methionine and nutrient starvation, are capable of activating the pathway via a G-protein coupled receptor, Gpr4 (22–24). Mutants lacking Pka1, the catalytic subunit of PKA, show a reduction in levels of capsule and melanin formation, along with sterility and virulence attenuation, in a mouse model of cryptococcosis (19, 25). In contrast,

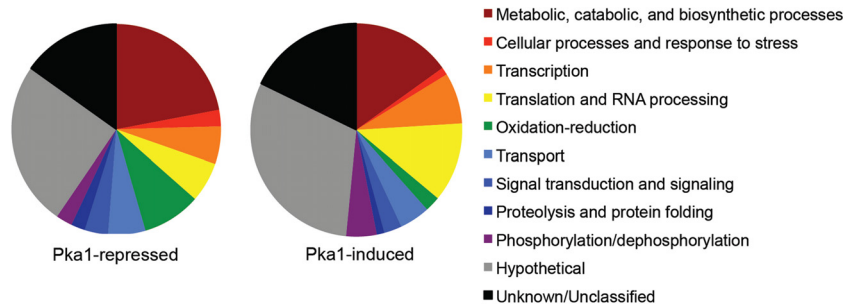


FIG 1 Modulation of Pka1 expression changes the proteome profile of *C. neoformans*. The pie charts indicate unique proteins identified and quantified under Pka1-repressed conditions (glucose-containing medium) and Pka1-induced conditions (galactose-containing medium) and categorized according to their GO term biological classifications (shown on the right).

loss of Pkr1, the regulatory subunit of PKA, results in cells with an enlarged-capsule phenotype and hypervirulence (19).

In general, the underlying mechanisms and targets of cAMP/PKA regulation of virulence in *C. neoformans* remain to be characterized in detail. The influence of the cAMP pathway on the transcriptome was initially characterized by profiling a mutant defective in the Gpa1 $G\alpha$ protein that activates adenylate cyclase (26). That work revealed pathway regulation of genes for capsule assembly and the genes encoding laccases for melanin formation. The influence of PKA on the transcriptome was also studied with *pka1* Δ and *pkr1* Δ mutants (16). That analysis revealed an influence of PKA on transcript levels for genes related to cell wall synthesis, transport, metabolism, and glycolysis, as well as for genes encoding ribosomal proteins, stress and chaperone functions, and components of the secretory pathway. Importantly, PKA has been shown to influence capsule attachment to the cell wall via regulation of the pH-responsive transcription factor Rim101, a key regulator of cell wall functions (27). The recent construction and characterization of galactose-inducible and glucose-repressible versions of *PKA1* in *C. neoformans* by inserting the *GAL7* promoter upstream of the gene provides a further opportunity to investigate the influence of PKA activity on virulence traits (28). The initial use of the regulated strains showed that galactose induction of *PKA1* influences capsule thickness, cell size, ploidy, vacuole enlargement, and melanization and laccase activity, as well as the secretion of proteases and urease. The galactose-inducible and glucose-repressible *P_{GAL7}::PKA1* strain was also used recently to characterize changes in the secretome of *C. neoformans* in response to modulation of *PKA1* expression (29).

In the present study, we used the *P_{GAL7}::PKA1* strain to investigate the influence of *PKA1* modulation on the intracellular proteome. Specifically, we employed quantitative proteomics to analyze protein abundance, and we identified 302 proteins that were regulated by Pka1 and that covered a broad spectrum of biological processes. Through enrichment and bioinformatic analyses and an interactome study, we discovered a conserved pattern of regulation by Pka1 for proteins associated with translation, the ubiquitin-proteasome pathway (UPP), metabolism, amino acid biosynthesis, and virulence-related functions. The Pka1 influence on the UPP in *C. neoformans* was particularly striking because of the established connection between this pathway, PKA activity, and protein degradation in chronic neurodegenerative disorders and other human diseases. These diseases are associated with impaired protein turnover and the accumulation of intracellular

ubiquitin-protein aggregates, which are linked to changes in PKA activity (30, 31). We investigated the role of the proteasome further in *C. neoformans* by using the inhibitor bortezomib to confirm the connection with PKA and to demonstrate a reduction in both capsule production and fungal growth. Bortezomib is an FDA-approved, boronic acid-based proteasome inhibitor that is widely used as an anticancer drug for the treatment of multiple myeloma (32). In parallel, we also established that strains with altered PKA expression or activity have altered susceptibility to tunicamycin, thereby revealing a connection with endoplasmic reticulum (ER) stress. Overall, this study advanced our understanding of the influence of the cAMP/PKA pathway on the cryptococcal proteome and identified proteostasis as a potential therapeutic avenue for the treatment of cryptococcosis.

RESULTS

Quantitative profiling of the proteome upon modulation of *PKA1* expression. Given the virulence defect of a *pka1* mutant and Pka1 regulation of secreted virulence factors in *C. neoformans*, we hypothesized that Pka1 influences the abundance of proteins associated with these functions as well as general processes such as translation and metabolism (19). We therefore evaluated the effect of Pka1 regulation on the proteome by collecting cells of the wild-type (WT) and *P_{GAL7}::PKA1* strains grown under Pka1-repressed (glucose) and Pka1-induced (galactose) conditions at 16 h postinoculation (hpi). To account for any changes associated with the use of different carbon sources (glucose versus galactose) to repress or induce *PKA1* expression, the WT strain was grown under the same conditions and comparisons were performed between strains from the same carbon source. We analyzed the samples using quantitative mass spectrometry and identified 3,222 proteins representing 48.1% of the 6,692 predicted proteins from the genome sequence (33). A total of 1,453 and 1,435 proteins were identified and quantified by dimethyl labeling in two or more replicates under Pka1-repressed and Pka1-induced conditions, respectively; 1,176 proteins were found under both conditions. A comparison of Gene Ontology (GO) biological-classification terms for the unique cellular proteins identified under either repressed conditions (277 proteins) or induced conditions (259 proteins) revealed changes in the proteome profiles in the strains responding to modulation of Pka1 activity (Fig. 1). The majority of proteins under both repressed and induced conditions (61% and 63%, respectively) were associated with metabolic, catabolic, and biosynthetic processes or were unknown or unclassified (in-

cluding hypothetical proteins) (Fig. 1). Overall, the analysis of protein abundance in the *PKA1*-modulated strain revealed an impact of Pka1 on a diverse array of cellular processes.

Identification of Pka1-regulated proteins. We next identified the proteins regulated by Pka1 within the set of 1,176 proteins that were quantified and shared under the repressed and induced conditions. We examined the list of shared proteins and found 302 that passed a nonadjusted Student's *t* test with regard to altered abundance in response to Pka1 regulation (see Table S1 in the supplemental material). We also adjusted the significance levels to account for the multiple-testing hypothesis, and this more stringent analysis revealed 40 Pka1-regulated proteins with the highest statistical significance; these proteins are indicated with asterisks in the tables in this article. The broader set of 302 Pka1-regulated proteins identified in our analysis covered a diverse spectrum of GO term biological classifications (14 categories), including metabolic, catabolic, biosynthetic, and cellular processes, transcription and translation, proteolysis and protein folding, oxidation-reduction, response to stress, transport, phosphorylation/dephosphorylation, signaling and signal transduction, hypothetical proteins, and unknown/unclassified proteins. A density plot comparing the proteins identified under Pka1-repressed and Pka1-induced conditions highlighted the influence of modulation of Pka1 activity. Remarkably, this approach revealed that the majority of regulated proteins decreased in abundance upon induction of *PKA1* (Fig. 2A). A closer inspection of the GO term biological processes confirmed that the majority of the proteins in all 14 categories showed a decrease in abundance upon *PKA1* induction (Fig. 2B). In contrast, induction of *PKA1* expression caused an increase in protein abundance for only a small number of proteins in the same categories of metabolic and biosynthetic processes, proteolysis and protein folding, and phosphorylation/dephosphorylation, as well as for hypothetical, unknown, or unclassified proteins (Fig. 2B). The overall patterns were supported by additional analyses performed using GO term classifications and enrichment, as well as KEGG pathway analysis (see Fig. S1 and Tables S1, S2, and S3 in the supplemental material).

Several clusters of interactions are predicted by network mapping of Pka1-regulated proteins. Given the diverse impacts of Pka1 on the *C. neoformans* proteome, including components of several metabolic pathways and cellular processes, we next evaluated the predicted interaction network of Pka1-regulated proteins using the STRING (Search Tool for Retrieval of Interacting Genes/Proteins) database. We mapped the identified Pka1-regulated proteins and found that 1,509 protein-protein interactions were predicted (Fig. 3). Several clusters of protein-protein interactions were prominent in the interaction network map, with the greatest number occurring among proteins associated with the ribosome and translation (Table 1; see also Table S3 in the supplemental material). A second interaction cluster included proteins associated with the ubiquitin-proteasome pathway (UPP). Although this category was noted in the KEGG analysis, the network mapping highlighted the prominence of these proteins and revealed their association in the network with the proteins for translation (Table 2). Additional clusters in the network were more diverse and included interactions between proteins associated with metabolic and biosynthetic processes, phosphorylation/dephosphorylation, oxidation-reduction, and other functions. Interactions were also predicted for proteins in categories associated with stress, signaling, secretion, and virulence (Table 3). This group

also included proteins with functions in protein sorting and folding, e.g., an ortholog of the chaperone GrpE, a prefoldin alpha subunit, and a peptidyl-prolyl *cis-trans*-isomerase. With regard to virulence functions, our analysis revealed PKA regulation of the Cig1 protein (heme acquisition) and an acid phosphatase, both of which were previously observed in the PKA-regulated secretome, as well as chaperones, catalase, urease, and a superoxide dismutase (29, 34–37). Assays of the latter two enzymes and immunoblot analysis performed with anti-Hsp70 antibody supported the observed differences in the proteome data (see Fig. S2A, B, and C in the supplemental material). Similarly, our previous finding (that Pka1 induction reduced secreted urease activity) was consistent with the lower protein level for the enzyme observed in the current proteome analysis (Table 3) (28). Protein-protein interactions were not predicted for ~85 proteins in the data set. In general, the protein-protein interaction network for Pka1-regulated proteins emphasized the significant impact of Pka1 on the regulation of ribosomal proteins and translation, the UPP, and metabolism. Furthermore, the diverse classification of hypothetical proteins provided an opportunity for novel protein discovery in the context of PKA regulation of the proteome.

Characterization of Pka1-regulated novel proteins. Our quantitative proteomic analysis revealed that 64 (21%) of the 302 candidates for Pka1-regulated proteins were conserved hypothetical proteins. To better understand the potential functions of these proteins, we used bioinformatic analyses to predict subcellular location, secretion, protein function, and possible enzymatic classification and to identify homologues (see Table S4 in the supplemental material). The subcellular location prediction tools TargetP and TMHMM identified 14 proteins associated with the mitochondrion, along with one protein containing a transmembrane helix. We noted that mitochondrial functions also appeared prominently among the metabolic and biosynthetic proteins. None of the hypothetical proteins contained a predicted glycosylphosphatidylinositol (GPI) anchor, and only one contained an N-terminal signal peptide for conventional secretion. ProtFun identified proteins with cellular roles related to central intermediary metabolism, energy metabolism, amino acid biosynthesis, biosynthesis of cofactors, translation, regulation and transcription, regulatory functions, transport and binding, purines and pyrimidines, and the cell envelope. Forty candidate enzymes were identified, and eight were classifiable as lyases, three as ligases, and three as isomerases. Additional GO term categories were associated with growth factors, hormones, transcription and transcriptional regulation, immune response, voltage-gated ion channels, and structural proteins. Lastly, HMMER identified protein homologues, including NAD-, RNA-, and carbohydrate-binding proteins, enzymes (methyltransferase, glutathione-S-transferase, phosphatases, and a protein tyrosine kinase), a heat shock protein, translation/ribosomal proteins, and proteins associated with transcription and transcriptional repression. These results revealed a diverse classification of hypothetical proteins, along with the potential for novel protein discovery in the context of PKA regulation of the proteome. Interestingly, the two Hsp12 homologues that we identified are known to influence growth on amphotericin B and to be regulated by the cAMP and high-osmolarity glycerol (HOG) signaling pathways in *C. neoformans* (16, 38). Some of the identified proteins may also contribute to virulence and proliferation in vertebrate hosts. For example, this may be the case for CNAG_03007, which is a homologue of the CipC protein, because

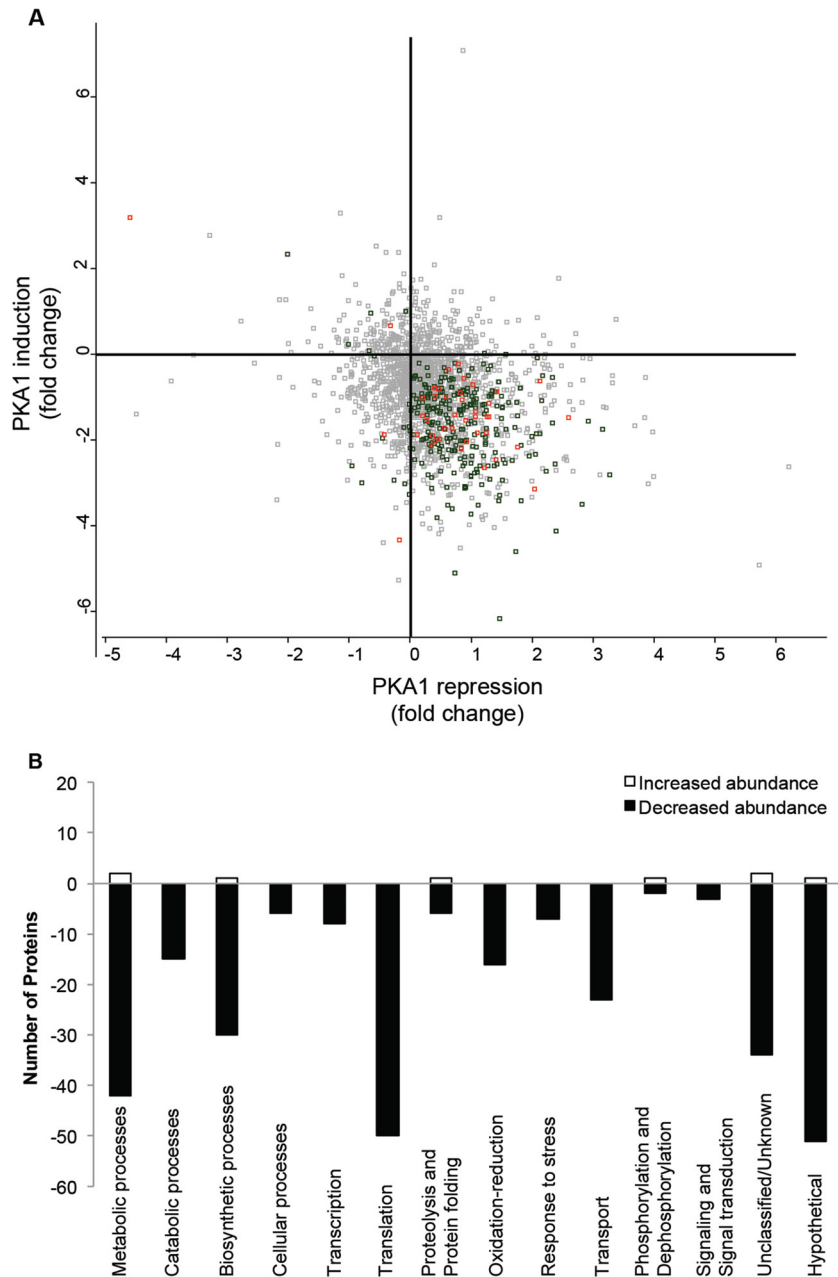


FIG 2 Modulation of Pka1 expression influences the abundance of 302 proteins. (A) Density scatterplot of proteins whose abundance changed upon repression or induction of *PKA1* expression. Proteins were identified in two or more replicates under Pka1-repressed (glucose) conditions and Pka1-induced (galactose) conditions. Normalized fold change values for the $P_{GAL7}::PKA1$ strain versus the WT strain are presented. Statistical analysis performed using a Student's *t* test identified 302 proteins whose results were significantly different ($P < 0.05$) under the two sets of conditions (green labels). A subset of 40 of these proteins showed a significant difference following correction for multiple-hypothesis testing using the Benjamini-Hochberg method (FDR = 0.05) (red labels). (B) Numbers of Pka1-regulated proteins in different GO term categories that showed changes in abundance upon induction of *PKA1* expression. The proteins were classified based on GO terms for biological processes.

the corresponding transcript was previously found to be highly abundant in cryptococcal cells obtained from the central nervous system of infected rabbits (39).

Connections between inhibition of the proteasome, PKA, and capsule production. As mentioned above, we found that induction of Pka1 expression decreased the abundance of multiple components of the UPP in *C. neoformans*, perhaps as part of a PKA-regulated remodeling of proteostasis. Given that one of the

most dramatic consequences of elevated PKA activity is the enlargement of the polysaccharide capsule, we investigated the impact of a proteasome inhibitor, bortezomib, on capsule production in the WT strain, the *pka1Δ* and *pkr1Δ* mutants, and the $P_{GAL7}::PKA1$ strain. This analysis revealed a reduction in the diameter of cell-associated capsule for the WT strain, the *pkr1Δ* mutant, and the induced $P_{GAL7}::PKA1$ strain in the presence of the inhibitor (Fig. 4A and B). The cell sizes of the *pkr1Δ* mutant and

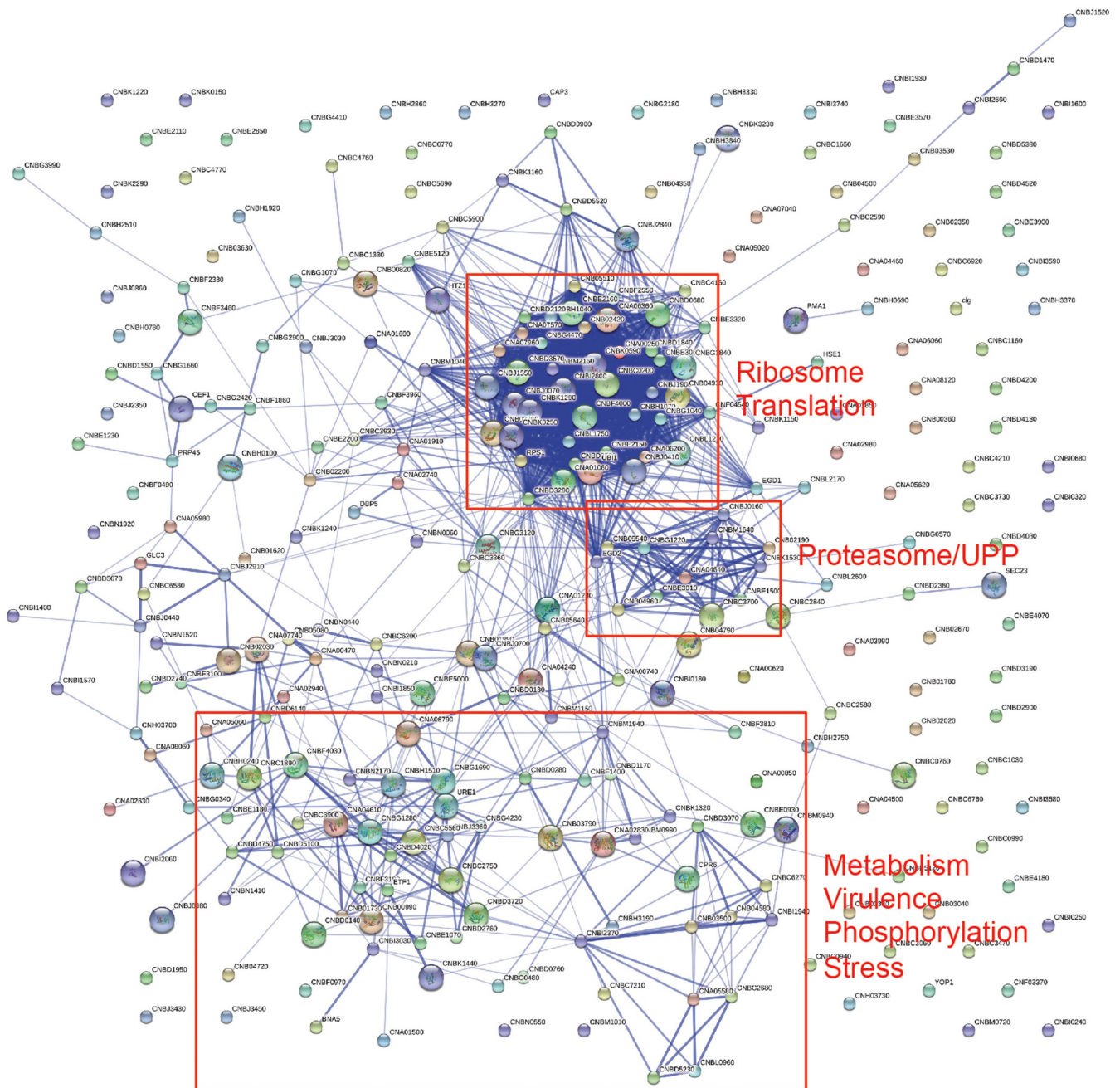


FIG 3 STRING analysis reveals an impact of Pka1 regulation on a diverse set of proteins as well as a prominent influence on translation and on the ubiquitin proteasome pathway. STRING was used to visualize predicted protein-protein interactions for the identified 300 Pka1-regulated proteins (<http://string-db.org>) using the corresponding proteins from *C. neoformans* strain JEC21 in the database (79). Several clusters were identified from the network mapping, and examples include (i) proteins associated with ribosomes and translation, including small-subunit ribosomal protein S13e (CNAG_01153) and eukaryotic translation initiation factor 3 subunit F (CNAG_06563); (ii) proteins associated with the proteasome, including 26S proteasome regulatory subunit N2 (CNAG_06175) and nascent polypeptide-associated complex subunit α (CNAG_04985); and (iii) diverse proteins associated with metabolism, virulence, and phosphorylation, including urease (CNAG_05540) and acetyl-coenzyme A (CoA) C-acetyltransferase (CNAG_02918). Nodes directly linked to the input are indicated with colors other than white, and nodes of a higher iteration/depth are indicated with white. Edges or predicted functional links consist of up to eight lines, with a different color representing each type of evidence (e.g., neighborhood, gene fusion, cooccurrence, coexpression, experiments, databases, text mining, and homology).

the induced $P_{GAL7}::PKA1$ strain were also decreased relative to the sizes of the WT cells upon treatment. No clear differences in capsule or cell size were observed in the absence of *PKA1* expression using the *pka1* Δ mutant strain and the $P_{GAL7}::PKA1$ strain grown under the repressed condition. These findings are consistent with

the previously observed changes in cell size upon modulation of *PKA1* expression (28). We also grew the WT strain, the *pka1* Δ mutant, and the $P_{GAL7}::PKA1$ strain in the presence of a range of bortezomib concentrations to identify the levels that were inhibitory for capsule formation (Fig. 4C). We found that capsule

TABLE 1 Proteins associated with translation and RNA processing in the Pka1-regulated proteome of *C. neoformans*

Gene ^a	Protein identification	Fold change ^b		P value ^c
		Pka1 repression	Pka1 induction	
CNAG_00034	Large-subunit ribosomal protein L9e	0.363	-1.034	0.021
CNAG_00116	Small-subunit ribosomal protein S3	0.694	-1.646	0.010
CNAG_00640	40S ribosomal protein S4	1.011	-2.183	0.013
CNAG_00656	Large-subunit ribosomal protein L7e	0.728	-2.201	0.049
CNAG_00779	Large-subunit ribosomal protein L27e	2.050	-0.797	0.048
CNAG_00819	Small-subunit ribosomal protein S30	1.667	-3.881	0.034
CNAG_01152	40S ribosomal protein s6	0.869	-1.200	0.008
CNAG_01153*	Small-subunit ribosomal protein S13e	0.950	-1.257	0.002
CNAG_01181	Small-subunit ribosomal protein S27Ae	2.252	-0.510	0.025
CNAG_01300	40S ribosomal protein S21	0.966	-2.924	0.045
CNAG_01332	Small-subunit ribosomal protein S24e	1.318	-2.812	0.040
CNAG_01455	Large-subunit ribosomal protein L39	1.359	-2.756	0.027
CNAG_01480	Large-subunit ribosomal protein L12	0.259	-1.889	0.048
CNAG_01843	Elongation factor Ts; mitochondrial	1.066	-1.523	0.027
CNAG_01884	Large-subunit ribosomal protein L3	1.305	-1.408	0.019
CNAG_01897	Bromodomain-containing factor 1	0.102	-0.604	0.012
CNAG_01951	Small-subunit ribosomal protein S22-A	1.879	-1.756	0.027
CNAG_01990	Small-subunit ribosomal protein S5	0.584	-1.195	0.032
CNAG_02145	Uncharacterized protein	0.848	-2.701	0.008
CNAG_02209	Nucleolar protein 56	0.291	-1.459	0.049
CNAG_02234	60S ribosomal protein L6	0.984	-2.161	0.041
CNAG_02330	Large-subunit ribosomal protein L21e	1.433	-1.945	0.017
CNAG_02331	Small-subunit ribosomal protein S9	1.492	-1.643	0.047
CNAG_02671	Pre-mRNA splicing factor CEF1	1.137	-2.223	0.012
CNAG_03198	40S ribosomal protein S8	0.949	-1.396	0.016
CNAG_03283	Large-subunit ribosomal protein L24e	1.577	-4.493	0.032
CNAG_03577	Large-subunit ribosomal protein LP0	0.332	-1.031	0.019
CNAG_03739	Large-subunit ribosomal protein L10-like	2.030	-3.596	0.027
CNAG_03747	Large-subunit ribosomal protein L27Ae	1.055	-2.462	0.046
CNAG_04004	40S ribosomal protein S1	1.442	-2.205	0.010
CNAG_04011	Large-subunit ribosomal protein L37a	1.441	-1.462	0.024
CNAG_04068	Large-subunit ribosomal protein L28e	1.210	-2.524	0.029
CNAG_04082	Proline-tRNA ligase	0.391	-0.988	0.026
CNAG_04445	Small-subunit ribosomal protein S7e	0.544	-2.111	0.048
CNAG_04448	Ribosomal protein L19	1.106	-2.674	0.014
CNAG_04609	Argonaute	0.864	-0.811	0.050
CNAG_04628	Eukaryotic translation initiation factor 6	1.085	-0.212	0.045
CNAG_04726	60S ribosomal protein L20	2.692	-2.196	0.022
CNAG_04762	Large-subunit ribosomal protein L4e	1.531	-2.273	0.034
CNAG_04883	Small-subunit ribosomal protein S18	0.760	-2.768	0.042
CNAG_05232	Large-subunit ribosomal protein L8	1.362	-2.096	0.031
CNAG_05416	Pre-mRNA processing protein 45	1.998	-1.781	0.020
CNAG_05525	Small-subunit ribosomal protein S26	2.900	-3.011	0.049
CNAG_05689	Pre-mRNA splicing factor SPF27	1.115	-1.774	0.034
CNAG_05762	Large-subunit acidic ribosomal protein P2	1.026	-0.994	0.021
CNAG_05904	Small-subunit ribosomal protein S14	2.288	-1.705	0.019
CNAG_06123	Leucine-tRNA ligase	0.352	-0.757	0.026
CNAG_06231	Large-subunit ribosomal protein L13	1.762	-2.044	0.045
CNAG_06563*	Eukaryotic translation initiation factor 3 subunit F	0.978	-1.397	0.001
CNAG_07839	Large-subunit ribosomal protein L11	2.105	-1.925	0.044

^a Gene designations labeled with an asterisk (*) represent genes that encoded proteins that gave significant results after multiple hypothesis testing (FDR, <0.05).

^b Data represent $P_{GAL7}::PKA1$ strain/WT strain normalized \log_2 average fold change values for three replicates determined under the respective glucose (repression) or galactose (induction) conditions.

^c Statistical analysis of Pka1 repression and Pka1 induction values was performed using Student's *t* test (*P* value, <0.05).

thickness was first noticeably impacted at 10 μ M bortezomib for the WT strain grown under both glucose and galactose capsule-inducing conditions. Conversely, capsule thickness and cell size remained unchanged for the *pkrl1* Δ mutant and the induced $P_{GAL7}::PKA1$ strain with a 10 μ M concentration of the inhibitor. A reduction in capsule and cell size was noted for these strains once the concentration of inhibitor reached 15 to 20 μ M, and a con-

centration of 25 μ M completely eliminated capsule production. Overall, these results are compatible with the conclusion that the regulatory connection between the cAMP/PKA signaling pathway and capsule formation includes a role for the UPP.

It is interesting that proteasome inhibition reduced capsule formation whereas PKA activation causes an enlarged capsule. These results suggest that a balance in the levels of expression of

TABLE 2 Proteins associated with the proteasome and ubiquitin pathways in the Pka1-regulated proteome of *C. neoformans*

Gene	Protein identification	Fold change ^a		P value ^b
		Pka1 repression	Pka1 induction	
CNAG_00136	Ubiquitin-activating enzyme E1	0.177	-1.216	0.006
CNAG_00180	Ubiquitin carboxyl-terminal hydrolase	1.090	-2.260	0.004
CNAG_00482	26S proteasome regulatory subunit N10	0.715	-1.531	0.028
CNAG_01861	26S proteasome non-ATPase regulatory subunit 10	0.569	-1.739	0.026
CNAG_01881	Molecular chaperone GrpE	1.557	-2.879	0.005
CNAG_01899	Prefoldin alpha subunit	1.574	-2.132	0.031
CNAG_02239	26S protease regulatory subunit 4	0.714	-2.185	0.035
CNAG_02725	20S proteasome subunit beta 2	0.594	-1.365	0.045
CNAG_02827	Ubiquitin-like protein Nedd8	0.764	-0.761	0.028
CNAG_03627	Peptidyl-prolyl <i>cis-trans</i> isomerase	0.648	-1.725	0.049
CNAG_03721	26S proteasome regulatory subunit N12	1.433	-2.933	0.049
CNAG_04014	26S proteasome regulatory subunit N9	0.379	-1.537	0.021
CNAG_04071	Proteasome subunit alpha type	1.093	-1.295	0.029
CNAG_04906	26S protease regulatory subunit 10B	0.519	-0.929	0.033
CNAG_06106	Chaperone regulator	-0.603	0.152	0.006
CNAG_06175	26S proteasome regulatory subunit N2	0.228	-2.166	0.031
CNAG_06602	Cysteine-type peptidase	1.580	-2.278	0.001
CNAG_07717	Ubiquitin carboxyl-terminal hydrolase	0.606	-0.705	0.003
CNAG_07719	26S protease regulatory subunit 7	0.168	-1.619	0.021

^a Data represent $P_{GAL7::PKA1}$ strain/WT strain normalized \log_2 average fold change values for three replicates determined under the respective glucose (repression) or galactose (induction) conditions.

^b Statistical analysis of Pka1 repression and Pka1 induction values was performed using Student's *t* test (*P* value, <0.05).

the UPP must be achieved by regulated PKA activity, perhaps in conjunction with regulation of translation, to properly orchestrate capsule production. To explore this possibility, we tested the translation inhibitor cycloheximide for an influence on capsule formation and found that although cell growth and capsule formation were inhibited, the cells eventually recovered their ability to make capsule (Fig. 4D). Interestingly, the observed recovery of capsule formation occurred even in the presence of a concentration of bortezomib that otherwise prevented capsule formation. Although additional biochemical studies are needed, these observations support the conclusion that a balance between protein synthesis and degradation has an impact on capsule formation.

The proteasome inhibitor bortezomib influences the growth of *C. neoformans* strains with altered PKA expression or activity. We next determined the influence of bortezomib on the growth of the WT and the $P_{GAL7::PKA1}$ strains, and on the growth of the *pka1Δ* and *pkr1Δ* mutants, in liquid media in the presence or absence of exogenous cAMP. Initially, we observed that the regulated $P_{GAL7::PKA1}$ strain showed slower growth than the WT strain in galactose medium without bortezomib but that it eventually reached a similar culture density by 72 h (Fig. 5A). This result suggests that the activation of *PKA1* expression negatively influences growth, possibly because of the reduction in the abundance of translation functions observed in the proteome analysis

TABLE 3 Identification of proteins associated with response to stress, chaperone function, signaling, and virulence in the Pka1-regulated proteome of *C. neoformans*

Gene ^a	Protein identification	Fold change ^b		P value ^c
		Pka1 repression	Pka1 induction	
CNAG_01404	Hsp71-like protein	0.680	-1.014	0.007
CNAG_01446	Uncharacterized protein	1.639	-3.295	0.014
CNAG_01653*	Cytokine-inducing glycoprotein	-4.515	3.130	0.002
CNAG_01744	Phosphatase	0.934	-1.785	0.011
CNAG_01817*	Signal recognition particle receptor subunit alpha	0.967	-0.574	0.003
CNAG_02817	GTP-binding protein ypt2	0.872	-0.783	0.015
CNAG_03143*	Uncharacterized protein	1.239	-1.371	0.000
CNAG_03891	Hsp60-like protein	0.697	-0.770	0.021
CNAG_03985	Glutaredoxin	1.215	-2.359	0.009
CNAG_05218	Adenylyl cyclase-associated protein	1.294	-0.075	0.045
CNAG_05540	Urease	0.476	-1.777	0.033
CNAG_06208	Heat shock 70-kDa protein 4	0.844	-0.931	0.021
CNAG_06287	Glutathione peroxidase	0.746	-0.330	0.044

^a Gene designations labeled with an asterisk (*) represent genes that encoded proteins that gave significant results after multiple hypothesis testing (FDR, <0.05).

^b Data represent $P_{GAL7::PKA1}$ strain/WT strain normalized \log_2 average fold change values for three replicates determined under the respective glucose (repression) or galactose (induction) conditions.

^c Statistical analysis of Pka1 repression and Pka1 induction values was performed using Student's *t* test (*P* value, <0.05).

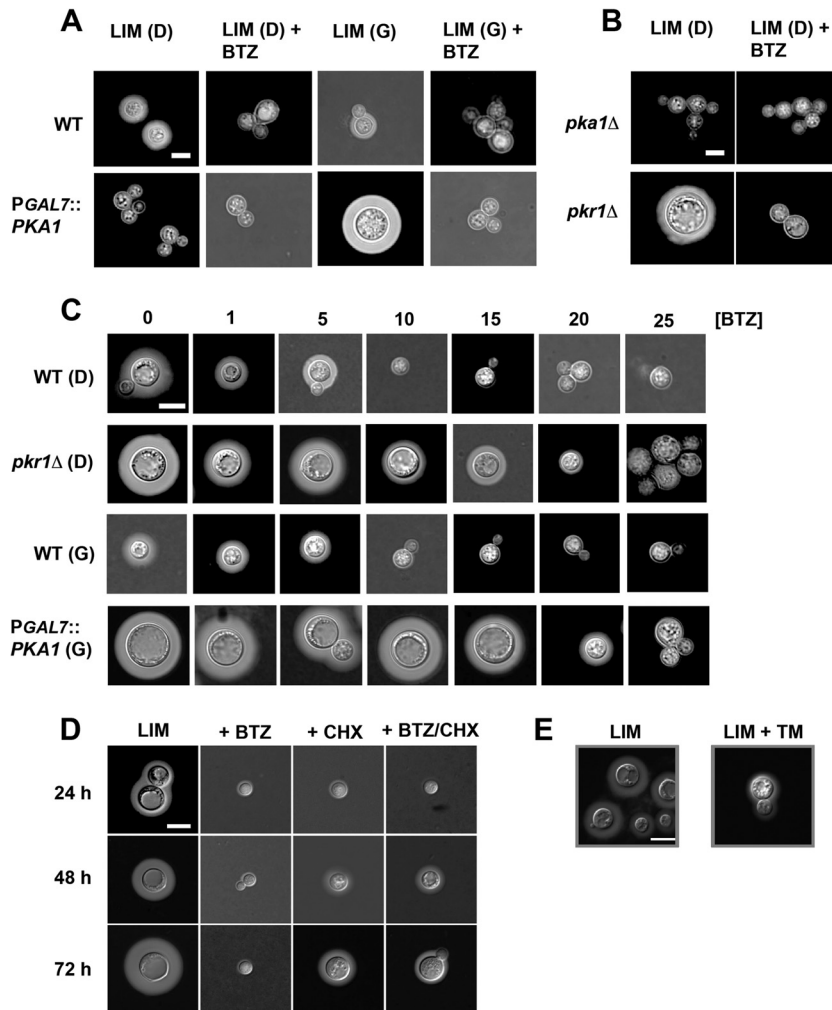


FIG 4 Inhibitors of the proteasome or of translation or glycosylation reduce capsule formation. Capsule diameter was examined with differential interference contrast (DIC) microscopy and India ink staining. (A) Capsule formation in the WT strain and the $P_{GAL7}::PKA1$ strain grown in low-iron medium (LIM) [either with glucose [LIM (D)] or with galactose [LIM (G)]] in the absence or presence of bortezomib (BTZ; 50 μ M). (B) Capsule formation in the $pka1\Delta$ and $pkrl1\Delta$ mutants in LIM (D) in the absence or presence of bortezomib (50 μ M). (C) Capsule formation was examined in the WT strain, the $pkrl1\Delta$ mutant, and the induced $P_{GAL7}::PKA1$ strain grown in LIM (D) or LIM (G) in the absence or presence of a range of bortezomib concentrations: 0, 1, 5, 10, 15, 20, and 25 μ M. Cells were incubated at 30°C for 48 h, mixed with India ink, and examined by DIC microscopy to visualize the capsule. (D) The WT strain was grown in LIM with or without 50 μ M bortezomib (New England Biolabs) and cycloheximide (CHX; 1 μ g/ml) for the times indicated. (E) The WT strain was grown in defined LIM in the absence or presence of tunicamycin (TM; 0.1 μ g/ml) after incubation for 24 h at 30°C. The bar indicates 10 μ m ($\times 100$ magnification).

(Table 1). The addition of bortezomib negatively impacted the growth of both the $P_{GAL7}::PKA1$ and WT strains, although substantial growth still occurred. In contrast, addition of both bortezomib and cAMP completely blocked the growth of both strains. These results indicated that activation of PKA by addition of cAMP enhanced susceptibility to bortezomib even in the regulated strain upon galactose-induced expression of $PKA1$. Similar results were observed when the two strains were grown with glucose as the carbon source (Fig. 5B). The two strains had the same growth profile in the absence of bortezomib (with or without cAMP), but addition of the drug again extended the lag phase and allowed eventual growth at the level seen with the untreated cultures. The inclusion of cAMP with bortezomib again eliminated the growth of both strains. Addition of cAMP alone did not influence the growth of any of the strains (data not shown).

The influence of bortezomib was examined further by compar-

ing the growth of a $pka1\Delta$ mutant lacking the main catalytic subunit to that of a $pkrl1\Delta$ mutant lacking the regulatory (cAMP-binding) subunit of PKA (Fig. 5C and D). The levels of growth of these strains were similar on galactose (Fig. 5C) and glucose (Fig. 5D) without additions, but treatment with bortezomib alone or in combination with cAMP almost completely eliminated the growth of the $pkrl1\Delta$ strain on either carbon source. In contrast, the $pka1\Delta$ strain in galactose or glucose media showed delayed growth on bortezomib, and the inclusion of cAMP caused a further delay. We note that the Pkr1 regulatory subunit and a second catalytic subunit, Pka2, are still present in the $pka1\Delta$ mutant. The responsiveness of the mutant may therefore indicate a contribution of Pka2 to the observed response to cAMP and bortezomib. Overall, these experiments demonstrated that bortezomib impairs the growth of *C. neoformans* and that activation of PKA by addition of exogenous cAMP or loss of the regulatory subunit of PKA

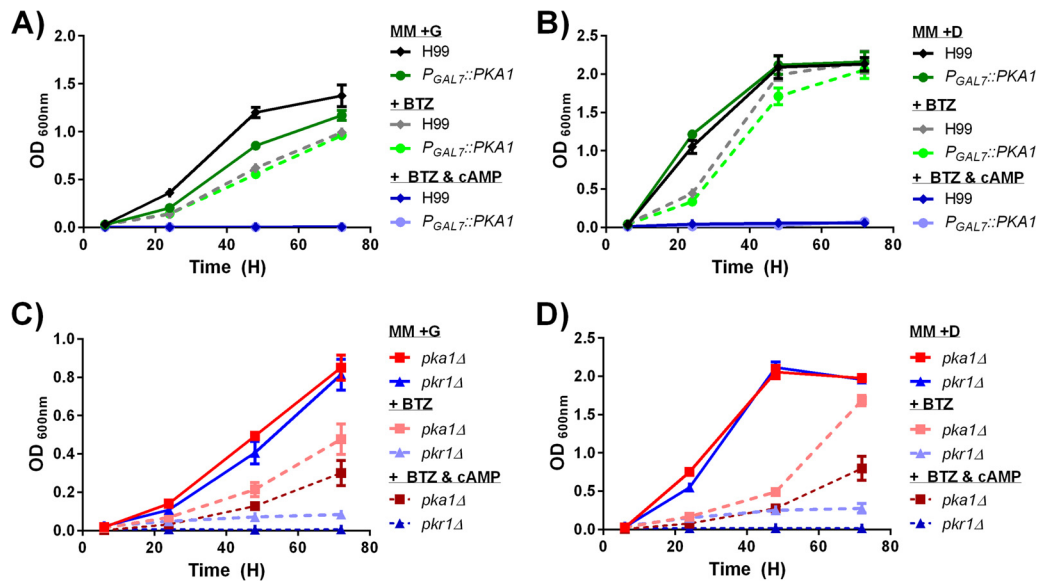


FIG 5 The proteasome inhibitor bortezomib impairs the growth of strains with altered PKA expression or activity. Growth assays were performed for the WT and *P_{GAL7}::PKA1* strains (A and B) and the *pka1Δ* and *pkrl1Δ* mutants (C and D) in liquid minimal medium with galactose (MM + G) (A and C) or glucose (MM + D) (B and D) at 37°C. Where indicated, bortezomib was added at 50 μ M and cAMP was added at 5 mM. Each experiment was performed a minimum of three times in triplicate. The averages and standard errors of data from an experiment representative of three replicates are shown for each time point.

increases susceptibility. In general, the regulated *P_{GAL7}::PKA1* strain may not be fully activated for PKA in galactose or fully repressed by glucose because addition of cAMP caused further growth inhibition by bortezomib. Additionally, this strain showed poorer growth with bortezomib in galactose medium versus glucose medium, suggesting that activation of *PKA1* expression increases susceptibility.

ER stress caused by tunicamycin impacts the growth of *C. neoformans* strains with altered PKA expression or activity. We next hypothesized that the observed influence of PKA on the abundance of proteins for translation and the UPP might be part of a larger impact of PKA activity on proteostasis and protein trafficking. We tested this theory by examining susceptibility to tunicamycin, an antibiotic that provokes ER stress by inhibiting the first step in the lipid-linked oligosaccharide pathway (40). Specifically, we tested the WT and the *P_{GAL7}::PKA1* strains, as well as the *pka1Δ* and *pkrl1Δ* mutants, in liquid media in the presence and absence of exogenous cAMP. Initially, we found that the regulated *P_{GAL7}::PKA1* strain again showed slower growth than the WT strain on galactose medium (Fig. 6A) as shown in Fig. 5A. The influence of growth on galactose appeared more pronounced in this experiment, perhaps due to the lower growth temperature (30°C) that was employed. The lower temperature was used because we noted that tunicamycin had a more pronounced influence on susceptibility at 30°C whereas the impact of bortezomib was greater at 37°C. Tunicamycin impaired the growth of both the WT and *P_{GAL7}::PKA1* strains on galactose, and addition of cAMP did not have a notable influence, although the growth of the strains was already minimal (Fig. 6A).

The WT and *P_{GAL7}::PKA1* strains grew to similar levels on glucose, and addition of tunicamycin (with or without cAMP) had only a slight negative impact on the growth of the regulated *P_{GAL7}::PKA1* strain but severely inhibited the WT strain (Fig. 6B). That is, a reduction in the expression of *PKA1* under conditions of growth

of the regulated strain in glucose eliminated the susceptibility to tunicamycin, suggesting that a low level of Pka1, perhaps resulting in low PKA activity, abrogated the ER stress provoked by the drug. In contrast, the growth of the WT strain was markedly impaired by addition of tunicamycin with or without cAMP. An influence of exogenous cAMP was not observed in this experiment, compared to similar treatment with bortezomib, and this may be because the growth of the WT strain was already quite impaired by treatment with tunicamycin. Importantly, a comparison of the levels of growth of the *P_{GAL7}::PKA1* strain on galactose (Fig. 6A) versus glucose (Fig. 6B) revealed a much greater inhibitory influence of tunicamycin under the inducing condition with galactose. We also observed that tunicamycin treatment reduced capsule elaboration, as also seen with bortezomib and cycloheximide (Fig. 4E).

We also tested the growth of the *pka1Δ* and *pkrl1Δ* mutants with or without tunicamycin and exogenous cAMP (Fig. 6C and D). Most notably, the *pkrl1Δ* mutant was quite susceptible to tunicamycin, with similar levels of impairment seen with and without cAMP on galactose or glucose medium. The *pka1Δ* strain showed slightly impaired growth in the presence of tunicamycin, and addition of cAMP actually improved the growth of the strain on galactose but not on glucose (compare Fig. 6C to D). This result could again indicate a potential role for Pka2 and/or an influence of Pkr1. It was noteworthy that added cAMP had little influence on the susceptibility of the *pka1Δ* mutant compared with its influence on bortezomib susceptibility for this strain, while the *pkrl1Δ* mutant was highly susceptible, as seen with bortezomib. In general, a reduction in PKA activity, in either the *pka1Δ* mutant or the *P_{GAL7}::PKA1* strain grown on glucose, protected the strains against ER stress provoked by tunicamycin. These results are consistent with the observed high susceptibility of the *pkrl1Δ* mutant to tunicamycin. Taken together, our results revealed that connections between ER stress caused by tunicamycin and the cAMP/

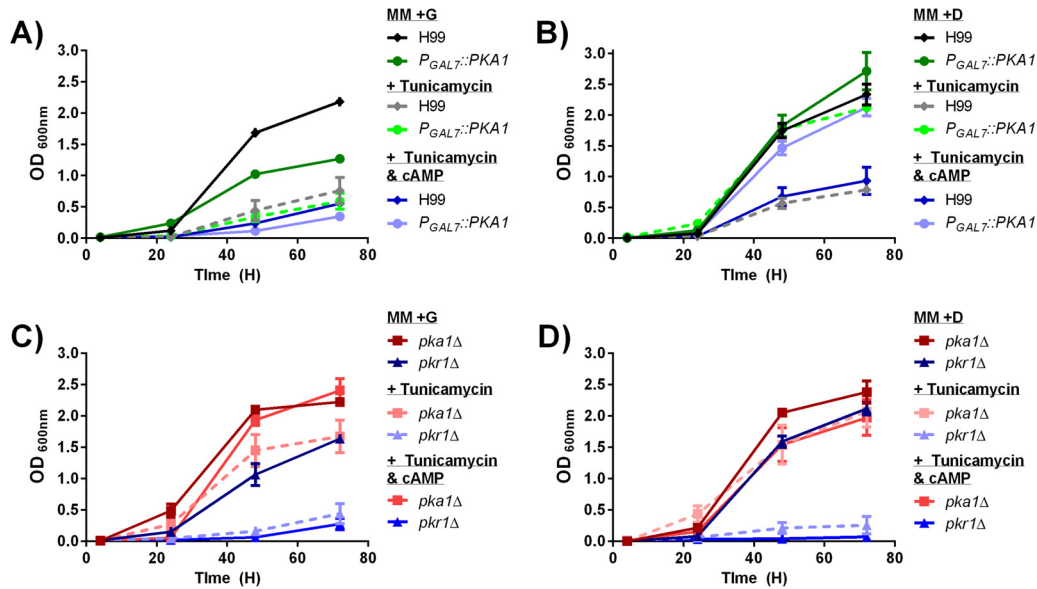


FIG 6 The glycosylation inhibitor tunicamycin impairs the growth of strains with altered PKA expression or activity. Growth assays were performed for the WT and *P_{GAL7}::PKA1* strains (A and B) and the *pka1Δ* and *pkrl1Δ* mutants (C and D) in liquid minimal medium with galactose (MM + G) (A and C) or glucose (MM + D) (B and D) at 30°C. Where indicated, tunicamycin was added at 0.5 μg/ml and cAMP was added at 1 mM. Each experiment was performed a minimum of three times in triplicate. The averages and standard errors of data from an experiment representative of three replicates are shown for each time point.

PKA pathway exist through the influence of the Pkr1 regulatory subunit on PKA activity or as a consequence of an additional function of Pkr1 and through the expression or activity of the Pka1 protein. Finally, we tested whether there was synergy between tunicamycin and bortezomib by using checkerboard assays to examine drug susceptibility (41). We did not observe synergy for these drugs or for bortezomib and fluconazole, an antifungal drug known to provoke ER stress (42 and data not shown).

Phenotypes of deletion mutants encoding PKA-regulated proteins. We compared our list of Pka1-regulated proteins with the *C. neoformans* gene deletion set to gain a more in-depth appreciation of the impact of *PKA1* modulation on the proteome (43, 44). In total, we linked our Pka1-regulated proteins with 59 deletion mutants that had previously been assessed for the production of virulence factors and growth at 37°C and that had been recently tested by chemical genetic analysis for sensitivity or resistance to small molecules (see Table S5 in the supplemental material) (43, 44). Of these 59 genes, the mutants encoded by 3 displayed a defect in melanin production, and the corresponding genes encoded a ubiquitin-like protein (CNAG_02827), a class E vacuolar protein-sorting machinery protein, HSE1 (CNAG_05882), and an uncharacterized protein (CNAG_01644) (43). These results are consistent with the known regulation of melanin production by PKA (19). Twenty-nine deletion mutants showed growth phenotypes, including sensitivity to H₂O₂, FeCl₃, sirolimus, and amphotericin B, upon challenge by small molecules. Several deletion strains displayed sensitivity to cell wall stressors, including SDS, Congo red, and caffeine, suggesting a role in cell wall integrity and potential capsule attachment. Mutants for several genes showed resistance to H₂O₂ or azole drugs such as fluconazole, suggesting roles for the proteins in protection against oxidative stress or ergosterol biosynthesis. These observations are interesting given the impact of redox activity on disulfide bond formation in the ER. Interestingly, three mutants showed an im-

part of ER stress triggered by tunicamycin. These mutants had defects in a translation-associated argonaute protein (CNAG_04609) or a glycosyl hydrolase (CNAG_05077) that enhanced susceptibility and in a phosphoketolase (CNAG_02230) that led to resistance. These observations further support the idea of a connection between PKA and ER function as well as of other potential links between PKA regulation and specific proteins that warrant further study.

DISCUSSION

The cAMP/PKA pathway plays a critical role in the virulence of *C. neoformans* because it regulates capsule and melanin formation (16, 17, 19). In this study, we used a quantitative proteomics approach to investigate the influence of *PKA1* expression on the proteome, and we identified 48.1% of the 6,692 predicted proteins from the genome sequence, including 1,453 and 1,435 under Pka1-repressed and Pka1-induced conditions, respectively. This level of protein identification is consistent with other proteome studies, including a recent examination of biofilm formation in *C. neoformans* (45). Remarkably, the major pattern of regulation observed upon induction of *PKA1* expression was a decrease in abundance for ribosomal and translational proteins, proteins associated with the UPP, and proteins associated with metabolism and biosynthesis. This regulatory pattern reflects an impact on proteostasis, and we found that strains with elevated PKA activity or expression were more susceptible to the anticancer drug and proteasome inhibitor bortezomib than the WT strain or strains with low PKA activity. These results are consistent with the identification of a PKA mutant in a screen for mutations causing synthetic lethality with bortezomib in *Schizosaccharomyces pombe* (46).

The impact of Pka1 regulation on translation. A key observation from this study was that induction of Pka1 suppressed the abundance of components of the translational machinery. Our

previous transcript profiling of *pka1* and *pkrl1* deletion mutants in *C. neoformans* also revealed a connection between Pka1 and expression of the translational machinery (16). We note, however, that other comparisons between our observed changes in protein abundance and transcript levels did not always reveal a correlation, perhaps because of differences in growth conditions and the strains (i.e., the *PKA1*-regulated strain versus the *pka1* Δ and *pkrl1* Δ mutants). The idea of the significance of the connection between cAMP/PKA signaling and translation in *C. neoformans* was recently bolstered by the characterization of Gib2, a protein that regulates cAMP levels via interaction with Ras1 and adenylyl cyclase (Cac1) and that is part of an interaction network with ribosomal proteins (47). The relationship between PKA and translation is interesting in the context of interactions between fungal pathogens and the phagocytic cells of vertebrate hosts. It is known, for example, that the phagocytosis of *C. neoformans* and *Candida albicans* by mammalian macrophages results in down-regulation of transcripts for the translational machinery (48, 49). More broadly, an influence of PKA on the expression of proteins involved in translation occurs in a number of fungi, including *C. albicans*, *Ustilago maydis*, and *Saccharomyces cerevisiae* (50–54). This regulation is best understood in *S. cerevisiae*, where nutritional signals influence the transcription of rRNA, as well as of genes for ribosome biogenesis and ribosomal proteins, via transcription factors controlled by the cAMP/PKA and target of rapamycin (TOR) pathways (55). Extensive studies in *S. cerevisiae* document PKA regulation of the translation machinery during the transient response to glucose as well as the unfolded protein response, the environmental stress response, autophagy, and yeast versus pseudohyphal/filamentous growth (50, 54, 55–58). The latter process may reflect a role for PKA on a longer time scale than that associated with its participation in the transient response to glucose (55). These other influences of PKA in *S. cerevisiae* may therefore be more relevant to the sustained activation expected from induction of *PKA1* expression in our experiments with *C. neoformans*. In particular, autophagy and the response to stress warrant further study.

Connections between PKA, translation, the UPP, and ER stress. Our observation of an influence of Pka1 expression on the abundance of UPP components is similar to an observed connection between PKA and proteostasis found in chronic neurodegenerative disorders and other diseases in humans. In this context, the UPP is a potential pharmacological target for the prevention and treatment of Alzheimer disease (AD), Parkinson disease (PD), Huntington disease (HD), and amyotrophic lateral sclerosis (ALS), as well as cardiovascular conditions such as hypertrophic and dilated cardiomyopathies and ischemic heart disease (30, 31, 59). All of these conditions are associated with impaired protein turnover and the accumulation of intracellular ubiquitin-protein aggregates (30, 31). For example, proteasome impairment is associated with lower PKA activity leading to progression of HD, and regulation based on positive feedback between PKA and the proteasome appears to be critical for HD pathogenesis (60, 61). Ribosomes also play important roles in cotranslational ubiquitination and quality control since newly synthesized polypeptides must be properly folded to avoid aggregation (60, 61). Specifically, a tiered system of quality control at the ribosome is responsible for proteostasis during protein synthesis that operates by sensing the nature of nascent protein chains, recruiting protein folding and translocation components, and integrating mRNA and nascent-

chain quality control (61). In this regard, we observed a reduction in the abundance of a number of chaperones (e.g., GrpE), proteins for sorting (e.g., prefoldin), a peptidyl-prolyl *cis-trans* isomerase, a subunit of the signal recognition particle receptor, and proteins for RNA processing. These observations suggest that a key role of Pka1 in *C. neoformans* is to regulate translation as well as functions for protein folding/sorting and the UPP machinery for degradation of misfolded proteins.

Given the observations described above, we hypothesize that the elevated Pka1 activity that occurs upon galactose induction of *P_{GAL7}::PKA1* expression may invoke ER stress and the unfolded protein response and, as a consequence, may change the requirements for proteasome activity and other processes related to proteostasis (62, 63). PKA activation in *C. neoformans* appears to suppress the abundance of proteins for these processes, perhaps as a mechanism to favor specific functions for the export of a large amount of capsule polysaccharide to the cell surface. It is curious, however, that galactose activation of *PKA1* expression in the *P_{GAL7}::PKA1* strain results in a large capsule and reduces the abundance of UPP proteins but inhibition of UPP activity with bortezomib impairs capsule formation. These observations suggest that a balanced regulation of PKA activity (and/or expression of *PKA1*) is needed for proper capsule production. The observation that cycloheximide also inhibits capsule formation but can allow production of a smaller capsule in the presence of bortezomib is consistent with the requirement for a balance. Moreover, the levels of free ubiquitin in the cell may be a component of the balance because studies in *S. cerevisiae* reveal that cycloheximide and proteasome inhibitors deplete ubiquitin by reducing translation and by promoting conjugation through the accumulation of substrates, respectively (64). Support for the idea of a connection with ubiquitin in *C. neoformans* comes from the observation that the effect of bortezomib treatment mimics the effect of a defect in the E3 ligase Fbp1 with regard to membrane integrity (65).

Our experiments with tunicamycin and bortezomib revealed an impact of both ER stress and proteasome inhibition on the growth of *C. neoformans* strains with altered PKA activity or expression. This was particularly prominent for the *pkrl1* Δ mutant, which is expected to have high PKA activity due to loss of the regulatory subunit of the enzyme. Both tunicamycin and bortezomib effectively shut down the growth of this mutant at concentrations that allowed growth of the WT strain. However, the addition of exogenous cAMP to ensure activation of PKA in the strains revealed two key differences with regard to susceptibility to bortezomib versus tunicamycin. First, the addition of cAMP to cultures of the WT or the *P_{GAL7}::PKA1* strains completely inhibited growth in the presence of bortezomib on media with galactose or glucose. Presumably, these conditions resulted in high PKA activity in the WT strain, leading to increased bortezomib susceptibility. The impact of cAMP on the *P_{GAL7}::PKA1* strain may reflect partial or eventual relief from glucose repression, leading to *PKA1* expression and/or potential activation of the second catalytic subunit, Pka2. In contrast, the *P_{GAL7}::PKA1* strain on glucose (with or without cAMP) showed greater resistance to tunicamycin than the WT strain (compare Fig. 5B to 6B). This result may indicate an alternative mechanism in which reduction in the level of Pka1 protein is the key factor in determining susceptibility to tunicamycin. Second, the addition of cAMP increased the susceptibility of the *pka1* Δ mutant to bortezomib on galactose and glucose while reducing and not influencing susceptibility to tunicamycin

on galactose and glucose, respectively. In the latter case, it is possible that addition of cAMP increased the activity of Pka2 in the *pka1Δ* mutant and caused increased susceptibility to bortezomib. The contributions of the Pka2 subunit are currently not well understood, although it was previously found that it did not contribute to virulence-related phenotypes (19, 25).

The inhibitor experiments also suggest that induction of *PKA1* expression in the regulated strain by galactose may not completely override the influence of Pkr1 and the requirement for elevated cAMP levels for full activation. Additionally, a clear distinction must be made between the influence of overexpressing Pka1 by galactose induction and activation of cAMP signaling leading to higher PKA activity. Pka1 overexpression might sequester Pkr1 and change its influence on downstream targets. We previously observed an increase in *PKR1* transcript levels upon galactose induction of *PKA1* expression, thus indicating further levels of regulation (16, 28). It is also possible that the Pka1 or Pkr1 proteins themselves influence ER function, as well as capsule synthesis and trafficking, and these may be independent of PKA activity. Together, these observations may explain phenotypic dissimilarities between the regulated strain and the *pkr1Δ* mutant beyond possible differences in the extent or duration of PKA activation in the two strains.

Bortezomib is known to display synergy with other chemotherapeutic agents, and it has been used to restore sensitivity to chemotherapy for resistant cancer cells (32, 66). In this context, it is interesting that a synergistic interaction of bortezomib with fluconazole was previously reported for *C. albicans* (67). Although we did not observe similar synergy for *C. neoformans*, the effect of bortezomib on growth and capsule formation suggests that further investigation of combinations with other drugs is warranted. We also did not observe synergy between bortezomib and tunicamycin, although both of these drugs interact with PKA. The impact of tunicamycin on capsule formation suggests that it may be fruitful to test combinations of agents that provoke ER stress and modulators of cAMP signaling such as cAMP derivatives and phosphodiesterase inhibitors. In particular, ER function and aspects of ER stress may be useful targets for antifungal drug development given recent associations with virulence and drug susceptibility in *Aspergillus fumigatus* and *Candida glabrata* (68, 69). More generally, our proteome analysis, in combination with the inhibitor studies, revealed that proteostasis is a promising therapeutic target for the treatment of cryptococcosis.

MATERIALS AND METHODS

Fungal strains and culture conditions. *Cryptococcus neoformans* var. *grubii* wild-type strain H99 (WT), H99 *pka1Δ* and *pkr1Δ* mutants, and galactose-inducible *PKA1* strain *P_{GAL7::PKA1}* (19, 28) were used for the analyses. For regulation of *PKA1* expression, cells were grown in minimal medium (MM) containing either 0.27% glucose (MM + D) or 0.27% galactose (MM + G).

Preparation of protein extracts and peptides. Cellular fractions were processed in triplicate for total protein extraction as previously described (70). Protein concentration was determined using the BCA protein assay (Pierce), and an in-solution trypsin digestion was performed on the total cellular extracts. Digested peptides from cellular fractions were subjected to C18 STop and Go Extraction (STAGE) tips (71). Reductive dimethylation was performed for differential peptide labeling (72). Digested and purified peptides were further fractionated by strong cation exchange (SCX) chromatography.

Protein identification by LC-tandem MS (LC-MS/MS) and MS data analysis. Purified and SCX-fractionated peptides were analyzed using a linear-trapping quadrupole-orbitrap mass spectrometer (LTQ-Orbitrap Velos; Thermo Fisher Scientific) online coupled to an Agilent 1290 Series high-performance liquid chromatography (HPLC) system using a nano-spray ionization source (Thermo Fisher Scientific). MaxQuant 1.3.0.25 was used for the analysis and quantification of mass spectrometry data, with statistical analysis and data visualization performed using Perseus 1/3/09 (73–75). The search was performed against a database comprised of 6,692 protein sequences from the *C. neoformans* WT source organism (*Cryptococcus neoformans* var. *grubii* H99; <http://www.uniprot.org>). Data corresponding to experimentally determined fold changes for WT and *P_{GAL7::PKA1}* strains grown under conditions of Pka1 repression (glucose-containing medium) and Pka1 induction (galactose-containing medium) were normalized and converted to a log₂ scale, and the average fold change values and standard deviations were used for analysis. A Student's *t* test (*P* value, <0.05) was performed for cellular proteins identified under both Pka1-repressed and Pka1-induced conditions to evaluate the statistical significance of the data. Multiple-hypothesis testing correction was performed on the proteome data using the Benjamini and Hochberg method (false-discovery rate [FDR], <0.05) (76). Proteins were characterized with Gene Ontology (GO) terms using a local installation of Blast2GO (77). Of the 302 Pka1-regulated proteins identified, 300 proteins could be mapped to the *C. neoformans* JEC21 database for data analysis and visualization (78). STRING (Search Tool for Retrieval of Interacting Genes/Proteins; <http://string-db.org>) was used to visualize predicted protein-protein interactions for the 300 identified Pka1-regulated proteins (79). The mass spectrometry (MS) proteomics data have been deposited in the ProteomeXchange Consortium via the PRIDE partner repository with data set identifier PXD002727 (80).

Enzyme and inhibitor assays and immunoblot analysis. Enzymatic assays were performed in triplicate according to the protocol of the manufacturer (BioVision Inc.). Hsp70 was detected by immunoblot analysis using a monoclonal anti-mouse antibody (Thermo Scientific Pierce; 1:3,000 dilution) followed by enhanced chemiluminescence (ECL; Amersham) for visualization. The impact of bortezomib (BTZ), cycloheximide (CHX), and tunicamycin on capsule elaboration was investigated using visualization with India ink. The WT, *P_{GAL7::PKA1}*, *pka1Δ*, and *pkr1Δ* strains were grown overnight in 5 ml of yeast extract-peptone-dextrose (YPD) at 30°C. Subsequently, 1×10^5 cells/ml were inoculated into 200 μ l of low-iron medium (LIM) with glucose [LIM (D)] or LIM with galactose [LIM (G)] with or without 50 μ M bortezomib (New England Biolabs) and/or 1 μ g/ml of cycloheximide. Cultures were incubated at 37°C for up to 72 h. For tunicamycin, 1×10^5 cells/ml were inoculated in 5 ml of low-iron medium (LIM glucose with or without 0.1 μ g/ml of the drug) and incubated at 30°C for 24 h. LIM was prepared with 20 mM HEPES and 22 mM NaHCO₃ and glucose or galactose as the carbon source for the respective strains as previously described (16). After incubation, the capsule was visualized with India ink and examined by differential interference microscopy (DIC). A titration of bortezomib was also used to assess the lowest concentration capable of influencing capsule production. The WT and *P_{GAL7::PKA1}* strains and the *pkr1Δ* mutant were grown overnight at 30°C in 5 ml of YPD, and 1×10^5 cells were then used to inoculate 200 μ l of LIM (D) or LIM (G) with or without bortezomib (1 to 25 μ M). The cells were incubated at 30°C for 48 h, and the capsule was visualized with India ink using differential interference microscopy (DIC). All assays were performed a minimum of three times.

The influence of proteasome inhibition and ER stress on the growth of the WT, *P_{GAL7::PKA1}*, *pka1Δ*, and *pkr1Δ* strains was tested by adding bortezomib and tunicamycin, respectively, to growth medium. Briefly, strains were grown overnight at 30°C in 5 ml of YPD and the cells from 50 μ l of the overnight cultures were then washed and transferred to 5 ml of MM + D or MM + G and grown overnight at 30°C. Following the initial incubation, 1×10^5 cells/ml were used to inoculate 12 ml of MM + D or MM + G with or without 50 μ M bortezomib or 0.5 μ g/ml of tuni-

camycin. Growth assays were performed in triplicate at 37°C for bortezomib and 30°C for tunicamycin with optical density measurements at 600 nm (OD₆₀₀) every 24 h. Where indicated, adenosine 3',5'-cyclic monophosphate (cAMP; Sigma) was added to the growth medium at concentrations of 5 mM for the bortezomib assays and 1 mM for the tunicamycin assays. All assays were performed a minimum of three times in triplicate. Potential synergy between drugs was assessed by a checkerboard assay based on standardized methods proposed by the National Committee for Clinical Laboratory Standards (NCCLS) for broth microdilution antifungal susceptibility testing and as previously described (41, 81).

Additional details of the materials and methods used are available in the supplemental material.

SUPPLEMENTAL MATERIAL

Supplemental material for this article may be found at <http://mbio.asm.org/lookup/suppl/doi:10.1128/mBio.01862-15/-/DCSupplemental>.

Text S1, DOCX file, 0.01 MB.
Figure S1, PDF file, 0.3 MB.
Figure S2, PDF file, 0.2 MB.
Figure S3, PDF file, 0.2 MB.
Table S1, PDF file, 0.1 MB.
Table S2, PDF file, 0.1 MB.
Table S3, PDF file, 0.1 MB.
Table S4, PDF file, 0.1 MB.
Table S5, PDF file, 0.1 MB.

ACKNOWLEDGMENTS

We thank J. Choi for strain construction and G. Hu, M. Kretschmer, S. Michaud, N. Scott, and J. Moon for helpful discussions and technical assistance.

This work was supported by an NSERC fellowship to J.M.H.G., CIHR open operating grants to J.W.K. and L.J.F., and a Burroughs Wellcome Fund Scholar Award in Molecular Pathogenic Mycology (J.W.K.). L.J.F. is the Canada Research Chair in Quantitative Proteomics.

REFERENCES

- Mitchell TG, Perfect JR. 1995. Cryptococcosis in the era of AIDS—100 years after the discovery of *Cryptococcus neoformans*. *Clin Microbiol Rev* 8:515–548.
- Park BJ, Wannemuehler KA, Marston BJ, Govender N, Pappas PG, Chiller TM. 2009. Estimation of the current global burden of cryptococcal meningitis among persons living with HIV/AIDS. *AIDS* 23:525–530. <http://dx.doi.org/10.1097/QAD.0b013e328322ffac> <http://dx.doi.org/10.1097/QAD.0b013e328322ffac>.
- Bulmer GS, Sans MD, Gunn CM. 1967. *Cryptococcus neoformans*. I. Nonencapsulated mutants. *J Bacteriol* 94:1475–1479.
- Kwon-Chung KJ, Polacheck I, Popkin TJ. 1982. Melanin-lacking mutants of *Cryptococcus neoformans* and their virulence for mice. *J Bacteriol* 150:1414–1421.
- Rhodes JC, Polacheck I, Kwon-Chung KJ. 1982. Phenoloxidase activity and virulence in isogenic strains of *Cryptococcus neoformans*. *Infect Immun* 36:1175–1184.
- Kwon-Chung KJ, Rhodes JC. 1986. Encapsulation and melanin formation as indicators of virulence in *Cryptococcus neoformans*. *Infect Immun* 51:218–223.
- Polacheck I, Kwon-Chung KJ. 1988. Melanogenesis in *Cryptococcus neoformans*. *J Gen Microbiol* 134:1037–1041. <http://dx.doi.org/10.1099/00221287-134-4-1037>.
- Chang YC, Kwon-Chung KJ. 1994. Complementation of a capsule-deficient mutation of *Cryptococcus neoformans* restores its virulence. *Mol Cell Biol* 14:4912–4919. <http://dx.doi.org/10.1128/MCB.14.7.4912>.
- Coenjaerts FEJ, Walenkamp AME, Mwinzi PN, Scharringa J, Dekker HAT, van Strijp JAG, Cherniak R, Hoepelman AIM. 2001. Potent inhibition of neutrophil migration by cryptococcal mannoprotein-4-induced desensitization. *J Immunol* 167:3988–3995. <http://dx.doi.org/10.4049/jimmunol.167.7.3988>.
- Bose I, Reese AJ, Ory JJ, Janbon G, Doering TL. 2003. A yeast under cover: the capsule of *Cryptococcus neoformans*. *Eukaryot Cell* 2:655–663. <http://dx.doi.org/10.1128/EC.2.4.655-663.2003>.
- Walenkamp AME, Ellerbroek P, Scharringa J, Rijkers E, Hoepelman AIM, Coenjaerts FEJ. 2003. Interference of *Cryptococcus neoformans* with human neutrophil migration. *Trop Dis* 531:315–339. http://dx.doi.org/10.1007/978-1-4615-0059-9_27.
- Del Poeta M. 2004. Role of phagocytosis in the virulence of *Cryptococcus neoformans*. *Eukaryot Cell* 3:1067–1075. <http://dx.doi.org/10.1128/EC.3.5.1067-1075.2004>.
- Janbon G. 2004. *Cryptococcus neoformans* capsule biosynthesis and regulation. *FEMS Yeast Res* 4:765–771. <http://dx.doi.org/10.1016/j.femsyr.2004.04.003>.
- Shoham S, Levitz SM. 2005. The immune response to fungal infections. *Br J Haematol* 129:569–582. <http://dx.doi.org/10.1111/j.1365-2141.2005.05397.x>.
- Yoneda A, Doering TL. 2006. A eukaryotic capsular polysaccharide is synthesized intracellularly and secreted via exocytosis. *Mol Biol Cell* 17:5131–5140. <http://dx.doi.org/10.1091/mbc.E06-08-0701>.
- Hu G, Steen BR, Lian T, Sham AP, Tam N, Tangen KL, Kronstad JW. 2007. Transcriptional regulation by protein kinase A in *Cryptococcus neoformans*. *PLoS Pathog* 3:e42. <http://dx.doi.org/10.1371/journal.ppat.0030042>.
- Alspaugh JA, Perfect JR, Heitman J. 1997. *Cryptococcus neoformans* mating and virulence are regulated by the G-protein alpha subunit GPA1 and cAMP. *Genes Dev* 11:3206–3217. <http://dx.doi.org/10.1101/gad.11.23.3206>.
- Kozubowski L, Lee SC, Heitman J. 2009. Signalling pathways in the pathogenesis of *Cryptococcus*. *Cell Microbiol* 11:370–380. <http://dx.doi.org/10.1111/j.1462-5822.2008.01273.x>.
- D'Souza CA, Alspaugh JA, Yue C, Harashima T, Cox GM, Perfect JR, Heitman J. 2001. Cyclic AMP-dependent protein kinase controls virulence of the fungal pathogen *Cryptococcus neoformans*. *Mol Cell Biol* 21:3179–3191. <http://dx.doi.org/10.1128/MCB.21.9.3179-3191.2001>.
- Kronstad JW, Attarian R, Cadieux B, Choi J, D'Souza CA, Griffiths EJ, Geddes JMH, Hu G, Jung WH, Kretschmer M, Saikia S, Wang J. 2011. Expanding fungal pathogenesis: *Cryptococcus* breaks out of the opportunistic box. *Nat Rev Microbiol* 9:193–203. <http://dx.doi.org/10.1038/nrmicro2522>.
- McDonough KA, Rodriguez A. 2012. The myriad roles of cyclic AMP in microbial pathogens: from signal to sword. *Nat Rev Microbiol* 10:27–38. <http://dx.doi.org/10.1038/nrmicro2688>.
- Iraqi I, Vissers S, Bernard F, De Craene J, Boles E, Urrestarazu A, André B. 1999. Amino acid signaling in *Saccharomyces cerevisiae*: a permease-like sensor of external amino acids and F-box protein Grr1p are required for transcriptional induction of the AGP1 gene, which encodes a broad-specificity amino acid permease. *Mol Cell Biol* 19:989–1001. <http://dx.doi.org/10.1128/MCB.19.2.989>.
- Rohde JR, Cardenas ME. 2004. Nutrient signaling through TOR kinases controls gene expression and cellular differentiation in fungi. *Curr Top Microbiol Immunol* 279:53–72. http://dx.doi.org/10.1007/978-3-642-18930-2_4.
- Xue C, Bahn Y, Cox G, Heitman J. 2006. G protein-coupled receptor Gpr4 senses amino acids and activates the cAMP-PKA pathway in *Cryptococcus neoformans*. *Mol Biol Cell* 17:667–679. <http://dx.doi.org/10.1091/mbc.E05-07-0699>.
- Hicks JK, D'Souza CA, Cox GM, Heitman J. 2004. Cyclic AMP-dependent protein kinase catalytic subunits have divergent roles in virulence factor production in two varieties of the fungal pathogen *Cryptococcus neoformans*. *Eukaryot Cell* 3:14–26. <http://dx.doi.org/10.1128/EC.3.1.14-26.2004>.
- Pukkila-Worley R, Gerrald QD, Kraus PR, Boily MJ, Davis MJ, Giles SS, Cox GM, Heitman J, Alspaugh JA. 2005. Transcriptional network of multiple capsule and melanin genes governed by the *Cryptococcus neoformans* cyclic AMP cascade. *Eukaryot Cell* 4:190–201. <http://dx.doi.org/10.1128/EC.4.1.190-201.2005>.
- O'Meara TR, Norton D, Price MS, Hay C, Clements MF, Nichols CB, Alspaugh JA. 2010. Interaction of *Cryptococcus neoformans* Rim101 and protein kinase A regulates capsule. *PLoS Pathog* 6:e1000776. <http://dx.doi.org/10.1371/journal.ppat.1000776>.
- Choi J, Vogl AW, Kronstad JW. 2012. Regulated expression of cyclic AMP-dependent protein kinase A reveals an influence on cell size and the secretion of virulence factors in *Cryptococcus neoformans*. *Mol Microbiol*

- 85:700–715. <http://dx.doi.org/10.1111/j.1365-2958.2012.08134.x> <http://dx.doi.org/10.1111/j.1365-2958.2012.08134.x>.
29. Geddes JMH, Croll D, Caza M, Stoykov N, Foster LJ, Kronstad JW. 2015. Secretome profiling of *Cryptococcus neoformans* reveals regulation of a subset of virulence-associated proteins and potential biomarkers by protein kinase A. *BMC Microbiol* 15:206. <http://dx.doi.org/10.1186/s12866-015-0532-3>.
 30. Huang Q, Figueiredo-Pereira ME. 2010. Ubiquitin/proteasome pathway impairment in neurodegeneration: therapeutic implications. *Apoptosis* 15:1292–1311. <http://dx.doi.org/10.1007/s10495-010-0466-z>.
 31. Wang X, Li J, Zheng H, Su H, Powell SR. 2011. Proteasome functional insufficiency in cardiac pathogenesis. *Am J Physiol Heart Circ Physiol* 301:H2207–H2219. <http://dx.doi.org/10.1152/ajpheart.00714.2011>.
 32. Merin N, Kelly K. 2014. Clinical use of proteasome inhibitors in the treatment of multiple myeloma. *Pharmaceuticals* 8:1–20. <http://dx.doi.org/10.3390/ph8010001>.
 33. Janbon G, Ormerod KL, Paulet D, Byrnes EJ, III, Yadav V, Chatterjee G, Mullapudi N, Hon C, Billmyre RB, Brunel F, Bahn Y, Chen W, Chen Y, Chow EWL, Coppée J, Floyd-Averette A, Gaillardin C, Gerik KJ, Goldberg J, Gonzalez-Hilarion S, Gujja S, Hamlin JL, Hsueh YP, Ianiri G, Jones S, Kodira CD, Kozubowski L, Lam W, Marra M, Mesner LD, Mieczkowski PA, Moyrand F, Nielsen K, Proux C, Rossignol T, Schein JE, Sun S, Wollschlaeger C, Wood IA, Zeng Q, Neuvéglise C, Newlon CS, Perfect JR, Lodge JK, Idnurm A, Stajich JE, Kronstad JW, Sanyal K, Heitman J, Fraser JA, Cuomo CA, Dietrich FS. 2014. Analysis of the genome and transcriptome of *Cryptococcus neoformans* var. *grubii* reveals complex RNA expression and microevolution leading to virulence attenuation. *PLoS Genet* 10:e1004261. <http://dx.doi.org/10.1371/journal.pgen.1004261>.
 34. Cox GM, Harrison TS, McDade HC, Taborda CP, Heinrich G, Casadevall A, Perfect JR. 2003. Superoxide dismutase influences the virulence of *Cryptococcus neoformans* by affecting growth within macrophages. *Infect Immun* 71:173–180. <http://dx.doi.org/10.1128/IAI.71.1.173-180.2003>.
 35. Giles SS, Batinic-Haberle I, Perfect JR, Cox GM. 2005. *Cryptococcus neoformans* mitochondrial superoxide dismutase: an essential link between antioxidant function and high-temperature growth. *Eukaryot Cell* 4:46–54. <http://dx.doi.org/10.1128/EC.4.1.46-54.2005>.
 36. Lev S, Crosssett B, Cha SY, Desmarini D, Li C, Chayakulkeeree M, Wilson CF, Williamson PR, Sorrell TC, Djordjevic JT. 2014. Identification of Aph1, a phosphate-regulated, secreted, and vacuolar acid phosphatase in *Cryptococcus neoformans*. *mBio* 5:e01649-14. <http://dx.doi.org/10.1128/mBio.01649-14>.
 37. Olszewski MA, Noverr MC, Chen G, Toews GB, Cox GM, Perfect JR, Huffnagle GB. 2004. Urease expression by *Cryptococcus neoformans* promotes microvascular sequestration, thereby enhancing central nervous system invasion. *Am J Pathol* 164:1761–1771. [http://dx.doi.org/10.1016/S0002-9440\(10\)63734-0](http://dx.doi.org/10.1016/S0002-9440(10)63734-0).
 38. Maeng S, Ko YJ, Kim GB, Jung KW, Floyd A, Heitman J, Bahn YS. 2010. Comparative transcriptome analysis reveals novel roles of the Ras and cyclic AMP signaling pathways in environmental stress response and antifungal drug sensitivity in *Cryptococcus neoformans*. *Eukaryot Cell* 9:360–378. <http://dx.doi.org/10.1128/EC.00309-09>.
 39. Steen BR, Zuyderduyn S, Toffaletti DL, Marra M, Jones SJM, Perfect JR, Kronstad J. 2003. *Cryptococcus neoformans* gene expression during experimental cryptococcal meningitis. *Eukaryot Cell* 2:1336–1349. <http://dx.doi.org/10.1128/EC.2.6.1336-1349.2003>.
 40. Heifetz A, Keenan RW, Elbein AD. 1979. Mechanism of action of tunicamycin on the Udp-GlcNac-dolichyl-phosphate GlcNac-1-phosphate transferase. *Biochemistry* 18:2186–2192. <http://dx.doi.org/10.1021/bi00578a008>.
 41. National Committee for Clinical Laboratory Standards. 1997. Reference method for broth dilution antifungal susceptibility testing of yeasts. Approved standard M27-A. National Committee for Clinical Laboratory Standards, Wayne, PA.
 42. Bonilla M, Cunningham K. 2003. Mitogen-activated protein kinase stimulation of Ca²⁺ signaling is required for survival of endoplasmic reticulum stress in yeast. *Mol Biol Cell* 14:4296–4305. <http://dx.doi.org/10.1091/mbc.E03-02-0113>.
 43. Liu OW, Chun CD, Chow ED, Chen C, Madhani HD, Noble SM. 2008. Systematic genetic analysis of virulence in the human fungal pathogen *Cryptococcus neoformans*. *Cell* 135:174–188. <http://dx.doi.org/10.1016/j.cell.2008.07.046>.
 44. Brown JS, Nelson J, VanderSluis B, Deshpande R, Butts A, Kagan S, Polacheck I, Krysan D, Myers C, Madhani H. 2014. Unraveling the biology of a fungal meningitis pathogen using chemical genetics. *Cell* 159:1168–1187. <http://dx.doi.org/10.1016/j.cell.2014.10.044>.
 45. Santi L, Beys-da-Silva WO, Berger M, Calzolari D, Guimarães JA, Moresco JJ, Yates JR, III. 2014. Proteomic profile of *Cryptococcus neoformans* biofilm reveals changes in metabolic processes. *J Proteome Res* 13:1545–1559. <http://dx.doi.org/10.1021/pr401075f>.
 46. Takeda K, Mori A, Yanagida M. 2011. Identification of genes affecting the toxicity of anti-cancer drug bortezomib by genome-wide screening in *S. pombe*. *PLoS One* 6:e22021. <http://dx.doi.org/10.1371/journal.pone.0022021>.
 47. Wang Y, Shen G, Gong J, Shen D, Whittington A, Qing J, Treloar J, Boisvert S, Zhang Z, Yang C, Wang P. 2014. Noncanonical G beta Gib2 is a scaffolding protein promoting cAMP signaling through functions of Ras1 and Cacl1 proteins in *Cryptococcus neoformans*. *J Biol Chem* 289:12202–12216. <http://dx.doi.org/10.1074/jbc.M113.537183>.
 48. Fan W, Kraus PR, Boily MJ, Heitman J. 2005. *Cryptococcus neoformans* gene expression during murine macrophage infection. *Eukaryot Cell* 4:1420–1433. <http://dx.doi.org/10.1128/EC.4.8.1420-1433.2005>.
 49. Lorenz MC, Bender JA, Fink GR. 2004. Transcriptional response of *Candida albicans* upon internalization by macrophages. *Eukaryot Cell* 3:1076–1087. <http://dx.doi.org/10.1128/EC.3.5.1075-1087.2004>.
 50. Klein C, Struhl K. 1994. Protein kinase A mediates growth-regulated expression of yeast ribosomal-protein genes by modulating Rap1 transcriptional activity. *Mol Cell Biol* 14:1920–1928. <http://dx.doi.org/10.1128/MCB.14.3.1920>.
 51. Jones DL, Petty J, Hoyle D, Hayes A, Ragni E, Popolo L, Oliver S, Stateva L. 2003. Transcriptome profiling of a *Saccharomyces cerevisiae* mutant with a constitutively activated Ras/cAMP pathway. *Physiol Genomics* 16:107–118. <http://dx.doi.org/10.1152/physiolgenomics.00139.2003>.
 52. Jung WH, Stateva L. 2003. The cAMP phosphodiesterase encoded by CaPDE2 is required for hyphal development in *Candida albicans*. *Microbiology* 149:2961–2976. <http://dx.doi.org/10.1099/mic.0.26517-0>.
 53. Harcus D, Nantel A, Marcil A, Rigby T, Whiteway M. 2004. Transcriptional profiling of cyclic AMP signaling in *Candida albicans*. *Mol Biol Cell* 15:4490–4499. <http://dx.doi.org/10.1091/mbc.E04-02-0144>.
 54. Larraya LM, Boyce KJ, So A, Steen BR, Jones S, Marra M, Kronstad JW. 2005. Serial analysis of gene expression reveals conserved links between protein kinase A, ribosome biogenesis, and phosphate metabolism in *Ustilago maydis*. *Eukaryot Cell* 4:2029–2043. <http://dx.doi.org/10.1128/EC.4.12.2029-2043.2005>.
 55. Broach JR. 2012. Nutritional control of growth and development in yeast. *Genetics* 192:73–105. <http://dx.doi.org/10.1534/genetics.111.135731>.
 56. Jorgensen P, Rupes I, Sharom J, Schnepfer L, Broach J, Tyers M. 2004. A dynamic transcriptional network communicates growth potential to ribosome synthesis and critical cell size. *Genes Dev* 18:2491–2505. <http://dx.doi.org/10.1101/gad.1228804>.
 57. Marion RM, Regev A, Segal E, Barash Y, Koller D, Friedman N, O'Shea EK. 2004. Sfp1 is a stress- and nutrient-sensitive regulator of ribosomal protein gene expression. *Proc Natl Acad Sci U S A* 101:14315–14322. <http://dx.doi.org/10.1073/pnas.0405353101>.
 58. Kraft C, Deplazes A, Sohrmann M, Peter M. 2008. Mature ribosomes are selectively degraded upon starvation by an autophagy pathway requiring the Ubp3p/Bre5p ubiquitin protease. *Nat Cell Biol* 10:602–610. <http://dx.doi.org/10.1038/ncb1723>.
 59. Nijholt D, De Kimpe L, Elfrink H, Hoozemans J, Scheper W. 2011. Removing protein aggregates: the role of proteolysis in neurodegeneration. *Curr Med Chem* 18:2459–2476. <http://dx.doi.org/10.2174/092986711795843236>.
 60. Duttler S, Pechmann S, Frydman J. 2013. Principles of cotranslational ubiquitination and quality control at the ribosome. *Mol Cell* 50:379–393. <http://dx.doi.org/10.1016/j.molcel.2013.03.010>.
 61. Pechmann S, Willmund F, Frydman J. 2013. The ribosome as a hub for protein quality control. *Mol Cell* 49:411–421. <http://dx.doi.org/10.1016/j.molcel.2013.01.020>.
 62. Chang HJ, Jesch SA, Gaspar ML, Henry SA. 2004. Role of the unfolded protein response pathway in secretory stress and regulation of INO1 expression in *Saccharomyces cerevisiae*. *Genetics* 168:1899–1913. <http://dx.doi.org/10.1534/genetics.104.032961>.
 63. Glazier VE, Panepinto JC. 2014. The ER stress response and host tem-

- perature adaptation in the human fungal pathogen *Cryptococcus neoformans*. *Virulence* 5:351–356. <http://dx.doi.org/10.4161/viru.27187>.
64. Hanna J, Leggett DS, Finley D. 2003. Ubiquitin depletion as a key mediator of toxicity by translational inhibitors. *Mol Cell Biol* 23:9251–9261. <http://dx.doi.org/10.1128/MCB.23.24.9251-9261.2003>.
 65. Liu T-, Xue C, Deepe GS. 2014. Fbp1-mediated ubiquitin-proteasome pathway controls *Cryptococcus neoformans* virulence by regulating fungal intracellular growth in macrophages. *Infect Immun* 82:557–568. <http://dx.doi.org/10.1128/IAI.00994-13>.
 66. Dong B, Li H, Singh AB, Cao A, Liu J. 2015. Inhibition of PCSK9 transcription by berberine involves down-regulation of hepatic HNF1 alpha protein expression through the ubiquitin-proteasome degradation pathway. *J Biol Chem* 290:4047–4058. <http://dx.doi.org/10.1074/jbc.M114.597229>.
 67. Kaneko Y, Fukazawa H, Ohno H, Miyazaki Y. 2013. Combinatory effect of fluconazole and FDA-approved drugs against *Candida albicans*. *J Infect Chemother* 19:1141–1145. <http://dx.doi.org/10.1007/s10156-013-0639-0>.
 68. Richie DL, Hartl L, Aimaganianda V, Winters MS, Fuller KK, Miley MD, White S, McCarthy JW, Latgé J, Feldmesser M, Rhodes JC, Askew DS. 2009. A role for the unfolded protein response (UPR) in virulence and antifungal susceptibility in *Aspergillus fumigatus*. *PLoS Pathog* 5:e1000258. <http://dx.doi.org/10.1371/journal.ppat.1000258>.
 69. Miyazaki T, Kohno S. 2014. ER stress response mechanisms in the pathogenic yeast *Candida glabrata* and their roles in virulence. *Virulence* 5:365–370. <http://dx.doi.org/10.4161/viru.27373>.
 70. Crestani J, Carvalho PC, Han X, Seixas A, Broetto L, Fischer JdSdG, Staats CC, Schrank A, Yates JR, III, Vainstein MH. 2012. Proteomic profiling of the influence of iron availability on *Cryptococcus gattii*. *J Proteome Res* 11:189–205. <http://dx.doi.org/10.1021/pr2005296>.
 71. Rappsilber J, Ishihama Y, Mann M. 2003. Stop and go extraction tips for matrix-assisted laser desorption/ionization, nano-electrospray, and LC/MS sample pretreatment in proteomics. *Anal Chem* 75:663–670. <http://dx.doi.org/10.1021/ac026117i>.
 72. Boersema PJ, Aye TT, van Veen TAB, Heck AJR, Mohammed S. 2008. Triplex protein quantification based on stable isotope labeling by peptide dimethylation applied to cell and tissue lysates. *Proteomics* 8:4624–4632. <http://dx.doi.org/10.1002/pmic.200800297>.
 73. Cox J, Mann M. 2008. MaxQuant enables high peptide identification rates, individualized p.p.b.-range mass accuracies and proteome-wide protein quantification. *Nat Biotechnol* 26:1367–1372. <http://dx.doi.org/10.1038/nbt.1511>.
 74. Cox J, Matic I, Hilger M, Nagaraj N, Selbach M, Olsen JV, Mann M. 2009. A practical guide to the MaxQuant computational platform for SILAC-based quantitative proteomics. *Nat Protoc* 4:698–705. <http://dx.doi.org/10.1038/nprot.2009.36>.
 75. Cox J, Neuhauser N, Michalski A, Scheltema RA, Olsen JV, Mann M. 2011. Andromeda: a peptide search engine integrated into the MaxQuant environment. *J Proteome Res* 10:1794–1805. <http://dx.doi.org/10.1021/pr101065j>.
 76. Benjamini Y, Yekutieli D. 2001. The control of the false discovery rate in multiple testing under dependency. *Ann Statist* 29:1165–1188.
 77. Conesa A, Gotz S, Garcia-Gomez J, Terol J, Talon M, Robles M. 2005. Blast2GO: a universal tool for annotation, visualization and analysis in functional genomics research. *Bioinformatics* 21:3674–3676. <http://dx.doi.org/10.1093/bioinformatics/bti610>.
 78. Loftus BJ, Fung E, Roncaglia P, Rowley D, Amedeo P, Bruno D, Vamathevan J, Miranda M, Anderson I, Fraser J, Allen J, Bosdet I, Brent M, Chiu R, Doering T, Dontin M, D'Souza C, Fox D, Grinberg V, Fu J, Fukushima M, Haas B, Huang J, Janbon G, Jones S, Koo H, Krzywinski M, Kwon-Chung J, Lengeler K, Maiti R, Marra M, Marra R, Mathewson C, Mitchell T, Perteau M, Riggs F, Salzberg S, Schein J, Shvartsbeyn A, Shin H, Shumway M, Specht C, Suh B, Tenney A, Utterback T, Wickes B, Wortman J, Wye N, Kronstad J, Loftus BJ, et al. 2005. The genome of the basidiomycetous yeast and human pathogen *Cryptococcus neoformans*. *Science* 307:1321–1324. <http://dx.doi.org/10.1126/science.1103773>.
 79. Franceschini A, Szklarczyk D, Frankild S, Kuhn M, Simonovic M, Roth A, Lin J, Minguez P, Bork P, von Mering C, Jensen LJ. 2013. String v9.1: protein-protein interaction networks, with increased coverage and integration. *Nucleic Acids Res* 41:D808–D815. <http://dx.doi.org/10.1093/nar/gks1094>.
 80. Vizcaino JA, Deutsch EW, Wang R, Csordas A, Reisinger F, Rios D, Dienes JA, Sun Z, Farrah T, Bandeira N, Binz P, Xenarios I, Eisenacher M, Mayer G, Gatto L, Campos A, Chalkley RJ, Kraus H, Albar JP, Martinez-Bartolomé S, Apweiler R, Omenn GS, Martens L, Jones AR, Hermjakob H. 2014. ProteomeXchange provides globally coordinated proteomics data submission and dissemination. *Nat Biotechnol* 32:223–226. <http://dx.doi.org/10.1038/nbt.2839>.
 81. Barchiesi F, Schimizzi AM, Najvar LK, Bocanegra R, Caselli F, Di Cesare S, Giannini D, Di Francesco LF, Giacometti A, Carle F, Scalise G, Graybill JR. 2001. Interactions of posaconazole and flucytosine against *Cryptococcus neoformans*. *Antimicrob Agents Chemother* 45:1355–1359. <http://dx.doi.org/10.1128/AAC.45.5.1355-1359.2001>.